Speed of sound measurements of two binary natural gas mixtures (methane plus n-butane and methane plus isopentane) at cryogenic temperatures and in liquid phase

The Journal of Chemical Thermodynamics – Supplementary Material to the Paper

Speed of sound measurements of two binary natural gas mixtures (methane + n-butane and methane + isopentane) at cryogenic temperatures and in liquid phase.

G. Cavuoto[a], P. A. Giuliano Albo[a], S. Lago[a]

[a]*Istituto Nazionale di Ricerca Metrologica (INRiM), Strada delle Cacce 91, 10135 Torino, Italy*

1. Introduction

Natural gas is currently recognised as one of the most promising energy sources for meeting the challenges and issues arising from climate preservation and low-carbon emission policies. Because of its high energy density, compared to other fossil sources, gas releases much less CO_2 into the atmosphere when burned for the same amount of energy produced. In addition, the extensive and widespread natural gas distribution network, which includes both land transport by pipelines and sea transport by LNG (Liquefied Natural Gas) carriers, together with the extensive availability of already existing and functioning facilities all over the world, will be a key factor in the energy transition towards climate neutrality and the massive use of zero-emission or new-generation energy sources (e.g. green hydrogen and biomethane). All these aspects have made natural gas the energy source with the highest growth rate for primary energy production in recent decades [1] and its use is expected to keep increasing, especially in developing countries, until 2035 [2]. In this context of a steadily growing natural gas market, a more accurate thermodynamic characterisation of the gas mixtures, received and delivered at the entry and delivery points of the distribution networks, becomes crucial. In fact, the typical composition of natural gas is heterogeneous and, in general, is characterised by a prevalent content of methane, which normally amounts to more than 80 %, mixed with other heavier hydrocarbons (such as ethane, propane, butane, pentane) and, marginally, with other molecules (such as carbon dioxide, hydrogen sulphate, helium, nitrogen). Establishing the net energy content transferred, and thus the costs of buying and selling gas, is closely linked to the capability of accurately establishing the quality of the gas mixture, its volume or mass, its density, its specific heat, as well as the temperature and pressure at which it flows through the pipelines. The better the ability to measure or calculate these quantities, the better the ability to establish the exact energy content transported, thus limiting any discrepancies between the estimated gas sold and purchased. Against this background, oil and gas industries are interested in any methods and technological innovations that can improve the ability to carry out these measurements. In this regad, speed of sound is a thermodynamic property of gases that has proven to be useful for several reasons. Indeed, from accurate speed of sound measurements, which can be obtained in a non-invasive way and in prohibitive conditions (e.g. cryogenic temperatures or high pressures), it is possible to calculate, using derivative methods, other thermodynamic properties that would otherwise be very

Email address: g.cavuoto@inrim.it (G. Cavuoto)

difficult or impossible to measure directly [3 - 6]. In addition, it has been demonstrated that ultrasonic sensors specifically designed to work at cryogenic temperatures can provide traceable on-line speed of sound measurements useful for the calibration of industrial flowmeters installed along gas distribution lines or near regasification plants [7]. In this way, from accurate speed of sound measurements it would be possible to have a number of very cost-effective industrial benefits (e.g. on-line volume flow rate measurements can be calibrated much more frequently and cheaply, without prior knowledge of the gas mixture composition).

Typically, thermodynamic properties of a fluid are calculated from its equation of state, which is a function that determines the mutual dependence of temperature, pressure, density and composition in the thermodynamic equilibrium. In particular, the so-called fundamental gas equations of state, namely those equations expressed in terms of thermodynamic potentials, typically Gibbs or Helmholtz free energy, are of relevance since they allow, by means of derivative techniques, to obtain all the thermodynamic properties of a fluid over wide ranges of temperature and pressure. In order to ensure that these mathematical models are developed and improved with increasing reliability, it is necessary to have the widest possible range of experimental measurements of the thermodynamic properties of the fluid to be modeled. Among all the thermodynamic properties of a fluid, in particular density, specific heats, saturated vapour pressure and speed of sound, are universally acknowledged as the most advantageous and most essential physical quantities for the development of an equation of state [8, 9]. For the two natural gas mixtures (methane + isopentane and methane + n-butane) taken into account in this work, there are currently no experimental speed of sound measurements available, so those obtained and shown in this paper are the first ever obtained for these specific blends of gases and may therefore be useful in developing new specific equations of state for these mixtures or in improving existing ones already in use. In the context of natural gas, there are a number of equations of state which are industry standards for calculating the thermodynamic properties of gases and which are used in all processes to access to mixture properties, in measuring gas flows in the distribution network and in the calculations for billing the energy transported. Specifically, the *American Gas Association* (AGA) equation of state, AGA8-DC92 [10], is currently the ISO standard for estimating the density and compressibility factor of natural gas (used for the gas phase), while the *Groupe Européen de Recherches Gazières* fundamental equation of state, GERG-2008 [11], is adopted as the ISO standard (ISO 20765-2/3) for natural gas (valid for both gas and liquid phases). The latter is expressed in the Helmholtz free energy as a function of density, temperature and gas composition and is based on 21 components of the natural gas. Furthermore, in 2019 a new model was presented by Thol *et al*. for calculating the thermodynamic properties of LNGs, the EOS-LNG equation of state [12]. This model is based on the same mathematical expression used for GERG-2008, of which it is a potential successor, with the introduction of binary-specific functions for methane + n-butane, methane + isopentane, methane + n-pentane, and methane + isopentane.

In this work, we present and discuss experimental speed of sound measurements obtained for two binary mixtures of natural gas (98.998 mol% methane + 1.0021 mol% n-butane, 98.016 mol% methane + 1.984 mol% isopentane) in a temperature range between (100 and 160 K and for pressures up to 12 MPa. The experimental technique adopted was the *double pulse-echo*, which is widely accepted as

the most suitable technique for obtaining accurate speed of sound measurements for the liquid phase. Furthermore, measurements have been taken in both the supercritical and homogeneous liquid regions for both mixtures. The relative uncertainties associated with these measurements has been estimated to be between (0.28 and 0.37) %, depending on the different temperatures and pressures. Thus, the experimental results have been compared with the values predicted by the GERG-2008 model and EOS-LNG.

2. Experimental apparatus for cryogenic speed of sound measurements

The experimental apparatus used in this work has been designed by the authors and manufactured at INRiM specifically to ensure the best performance in terms of thermal control stability and accuracy of speed of sound measurements under cryogenic temperatures and high pressures. A detailed description of this apparatus can be found in [15], while the characterisation of the instrument through speed of sound measurements in liquid methane is described in [7], where the improvements later implemented in the apparatus are listed and the possibility of using the ultrasonic sensor as a transfer standard for traceable speed of sound measurements for industrial fluids at cryogenic temperatures is discussed. For the sake of completeness we will describe below the main components of the measuring instrument. The active sensor is an ultrasonic cell, shown in the Fig. 1, made of AISI 316L stainless steel. Its total length is 75 mm. An ultrasonic transducer, a ceramic piezoelectric, is located inside it, acting both as an emitter and receiver of the acoustic bursts generated by a function generator. This is placed in such a way as to divide the cell into two sections of different lengths, so that the acoustic paths thus obtained are of different lengths, L_1 and L_2. The transducer is excited with a series of 5-cycles, 10 V_{pp} amplitude

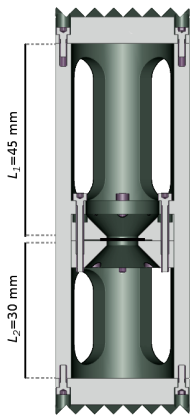

Figure 1: Cross section of the stainless steel cell used as an ultrasonic sensor for cryogenic speed of sound measurements.

sinusoidal electrical bursts, emitting an ultrasonic wave that propagates along the two acoustic paths. These ultrasonic pulses are reflected at the ends of the cell and the echoes are sampled by a digital oscilloscope at the rate of 5 gigasamples per seconds. In order to be able to correlate the two echoes, the shapes of the two sampled signals must be as similar as possible, so that they can be superimposed. Since the patterns of the signals change as the carrier excitation frequency of the transducer is changed,

the result is that, especially at lower pressures, the acoustic pulse travelling along the longer path can be distorted in such a way that it is sampled with a different number of cycles than that propagating along the shorter path. In this way the superposition of the two signals is no longer correct, as shown in Fig. 2 (a). This problem can be solved by varying the carrier frequency of the ultrasonic wave in order to find the best superposition of the two echoes, Fig. 2 (b). For this reason, the acoustic transducer is excited at

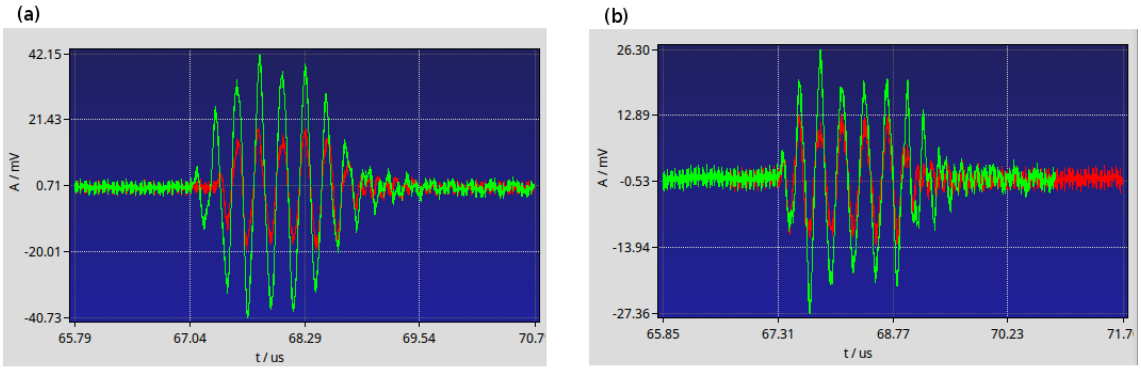

Figure 2: Superposition of two echoes sampled during a speed of sound measurement at $T = 120$ K and $p = 4$ MPa. The first signal (green) is the echo of the acoustic burst that travels the shorter path, the second (red) travels the longer path. Figure (a) shows the result of a 4 MHz excitation resulting in the two echoes being incorrectly overlapped; figure (b) shows the same measurement obtained with the carrier frequency changed to 3.5 MHz and the two echoes result correctly overlapped.

a carrier frequency that ranges between (3 and 4) MHz.

The temperature control system is shown in Fig. 3. The measuring cell (1 in Fig. 3) is housed inside an AISI-316L stainless steel pressure vessel (2 in Fig. 3), capable of operating up to 70 MPa. Cooling of the system to cryogenic temperatures is provided by liquid nitrogen flowing through an aluminium heat exchanger (3 in Fig. 3) and the thermal contact between it and the pressure vessel takes place by a temperature-controlled copper thermal bridge fitted between them. Finally, the sample fluid is injected into the system in its gaseous phase through an inlet line (4 in Fig. 3) sealed to the upper end flange of the high-pressure vessel.

The whole apparatus is suspended inside a vacuum chamber in order to be thermally isolated from the environment. This chamber is evacuated at a pressure of about $5{\cdot}10^{-3}$ mbar. The pressure of the sample fluid is measured by using a temperature controlled pressure transducer (Honeywell Super TJE) placed on the inlet line, just outside the upper flange of the vacuum chamber, and calibrated with an accuracy of ± 0.025 MPa, up to 50 MPa. Temperature of the sample is obtained as the mean value of the resistances measured by two PT100 placed inside the walls of the pressure vessel. Other two PT100 thermometers are installed, one inside the copper thermal bridge, with the function of control sensor for the PID control, and the second placed inside a second aluminium thermal bridge above the pressure vessel, with the function of thermal shield designed to limit as much as possible the thermal fluxes from the external environment to the inner part of the system. These thermometers are calibrated by using the international temperature scale ITS-90 [16], using the triple point of argon, the triple point of mercury and the triple point of water, as calibration points, with an expanded uncertainty of ± 0.02 K ($k = 2$).

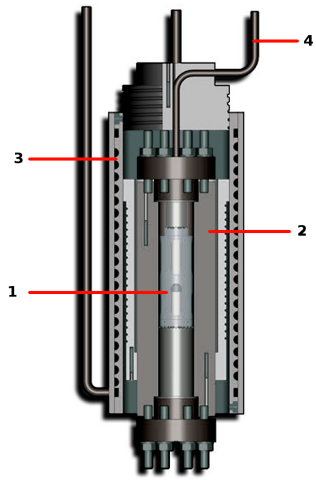

Figure 3: Scheme of the cryogenic thermal apparatus: (1) measuring cell; (2) pressure vessel; (3) heat exchanger; (4) gas inlet.

3. Measurement technique and corrections

The measurement technique adopted in this work is the *double pulse-echo* technique. This method has been chosen since it is recognised as a suitable and efficient way to obtain speed of sound measurements in fluids for liquid phase [17] (including natural gas mixtures at cryogenic temperatures). A detailed description of this experimental technique can be found in a variety of works reporting speed of sound measurements using the same transient technique under both homogeneous liquid and supercritical conditions. Among the numerous works available in the literature, it is worth mentioning the works of Benedetto *et al*. [18], for speed of sound in pure water in its liquid phase, of Javed *et al*. [19], where supercritical measurements were performed in several alcohols, the work of Lin *et al*. [20], where accurate speed of sound measurements and derived thermodynamic properties of pure water are shown, as well as the measurements in pure propane in the liquid and supercritical regions, provided by Meier *et al*. [21]. The working principle of this technique is based on the evaluation of the transit time τ an acoustic wave takes to travel along two opposite acoustic paths of different lengths, L_1 and L_2. Using a digital oscilloscope, the echoes of the acoustic bursts emitted and received back by the same piezoelectric acoustic transducer, after being reflected by two parallel reflectors are sampled. Thus, knowing the detailed patterns of these echoes, P_1 and P_1, it is possible to calculate the time-of-flight, or the time gap between the two echoes, by means of the correlation function:

$$C(\tau) = \int_{-\infty}^{+\infty} P_1(t)P_2(t+\tau)dt. \tag{1}$$

Indeed, the value τ_{exp} that maximizes the function $C(\tau)$, is precisely the time-delay between two consecutive echoes. Then, experimental speed of sound w_{exp} is calculated by measuring the difference of the paths length $\Delta L = L_2 - L_1$, as the ratio between the space $2\Delta L = 2(L_2 - L_1)$ and the time-of-flight τ_{exp}, between the two echoes:

$$w_{\text{exp}} = \frac{2\Delta L}{\tau_{\text{exp}}}. \tag{2}$$

To ensure the resulting experimental measurements satisfy the metrological standards for a reliable and accurate measurement, some corrections must be applied to compensate for side effects that would lead to uncorrect results.

3.1. Diffraction corrections

The first correction is related to the strictly acoustic effects deriving from the used measurement technique. In fact, the ultrasonic waves travelling through the sample fluid, after crossing the two acoustic paths and being received by the piezoelectric transducer, are subject to a phase shift that depends on the finite dimensions of the ultrasonic source. Since this phase shift depends mainly on the system geometry, specifically on the acoustic source diameter and on the overall acoustic path length, a first way to limit the diffraction effects as much as possible is to design the measurement cell in such a way that the corrections needed to correct these effects are small compared to other sources of uncertainty [22]. Furthermore, since a proper sizing of the measuring cell is not sufficient alone to totally prevent the possibility of a phase shift that would result in a delay in the measured time-of-flight, the following correction $\delta\tau$ must be applied to τ:

$$\delta\tau = \frac{\phi(2L_2) - \phi(2L_1)}{\omega_0}, \tag{3}$$

$$\phi(L) = \text{Arg}\left[1 - \exp\left(-\frac{i2\omega b^2/w_{\text{exp}}}{2L}\right)\left(\text{J}_0\left(\frac{2\omega b^2/w_{\text{exp}}}{2L}\right) + i\text{J}_1\left(\frac{2\omega b^2/w_{\text{exp}}}{2L}\right)\right)\right]. \tag{4}$$

where $\phi(L)$ is the phase shift as described in [23] and discussed in [24], b is the radius of the source, J_0 and J_1 are the Bessel functions of zero and first order, and $\omega = 2\pi f$ is the angular frequency, with f the carrier frequency of the acoustic wave.
Thus, the actual delay time $\tilde{\tau}$ is calculated as:

$$\tilde{\tau} = \tau_{\text{exp}} + \delta\tau. \tag{5}$$

3.2. Temperature gradient corrections

Since the time-of-flight is influenced not only by diffraction effects due to the undulatory motion of the acoustic waves, but also by thermal effects within the measurement system, it needs further correction. Specifically, due to the cryogenic temperatures involved in the experiment, thermal gradients within the measurement cell (and therefore along the acoustic paths) could grow so much that are no longer negligible. The following correction is needed, to obtain the time-delay τ_{g}, which occurs in the

presence of thermal gradients:

$$\tau_{\mathrm{g}} = \tau_{\mathrm{exp}} \left(1 + \frac{a}{\tau_{\mathrm{exp}} w_{\mathrm{exp}}^2} (L_2^2 - L_1^2) \right), \tag{6}$$

where the term a, which must be much smaller than the experimental speed of sound, w_{exp}, can be calculated as:

$$a = \frac{\partial w}{\partial z} = \frac{\partial w}{\partial T} \frac{\partial T}{\partial z}. \tag{7}$$

Hence, the term a, as shown in Eq. 7, depends on the sensitivity coefficient of w with respect to the temperature, T, and the temperature gradient along the direction z, which has conventionally been chosen to represent the longitudinal axis of the measuring cell. In order to prevent and limit this side effect caused by a thermal gradient, the thermal control system of the measuring system must be designed in such a way to minimise it. However, once the correction term for the thermal gradients has been determined, it is then possible to extend Eq. 5 to calculate the corrected value for the time of flight, $\widetilde{\tau}$, as follows:

$$\widetilde{\tau} = \tau_{\mathrm{exp}} + \delta\tau + \tau_{\mathrm{g}}, \tag{8}$$

where both the diffraction effects, $\delta\tau$, and the thermal gradient effects, τ_{g} have been taken into account.

3.3. Path length correction for temperature and pressure

In addition, due to the extreme conditions of temperature and pressure under which the measuring cell is subjected during the experiment, a further corrections to compensate for the deformations of the ultrasonic cell under diverse temperature and pressure conditions must be included. The variation of the cell length $\Delta L(T, p)$, specifically of the two acoustic paths L_1 and L_2, with respect to the results of calibration (performed at temperature T_0 and pressure p_0), can be calculated using the following expression:

$$\Delta L(T, p) = \Delta L(T_0, p_0) \left(1 + \alpha(T - T_0) - \frac{\beta_{\mathrm{T}}}{3} (p - p_0) \right), \tag{9}$$

where β_{T} and α are the isotermal compressibility and the thermal expansion coefficient of the AISI-316L stainless steel, the same material as the ultrasonic cell, respectively. The latter term is no longer constant when temperature is far below laboratory temperature, such as cryogenic temperatures. The values of the thermal expansion coefficients over a wide temperature range for several relevant materials are given in [25]. Using the values available for AISI-316L stainless steel, $\alpha(T)$ can be calculated by a polynomial fitting function as:

$$\alpha(T) = a + bT + cT^2 + dT^3, \tag{10}$$

where coefficients are a = 5.867532·10^{-7}, b = 1.405386·10^{-7}, c = 5.263604·10^{-10}, d = 7.604209·10^{-7}.

Then, under this condition, Eq. 9 becomes:

$$\Delta L(T,p) = \Delta L(T_0,p_0)\left(1 + \alpha(T)\exp(\gamma) - \frac{\beta}{3}(p - p_0)\right), \tag{11}$$

where $\gamma = a(T - T_0) + \frac{b}{2}(T^2 - T_0^2) + \frac{c}{3}(T^3 - T_0^3) + \frac{d}{4}(T^4 - T_0^4)$.

4. Gas mixtures characterisation and sample preparation

The two binary mixtures, methane + n-butane and methane + isopentane, considered in this work were prepared and delivered by the VSL (*Dutch Metrological Institute*). The gas mixtures have been produced from high-purity starting materials, in order to minimize any collateral effect due to the presence of possible impurities. The mole fractions of the components of both the gas mixtures have been calculated by comparison with the Dutch primary measurement standards by chromatography in accordance with ISO 6143 [26]. Table 1, showing the results of this analysis, reports the mole fractions of each component of the mixtures as certificated by the VSL, together with the associated expanded uncertainties (k = 2) of measurement, determined in accordance with the GUM (*Guide to the Expression of Uncertainty in Measurement*) [27]. Furthermore, since the sum of all components in the mixture expressed in mole fractions must be 100, the non-normalized values given in the calibration certificate have been normalized and reported in Table 1 as well.

Component	molar fraction (certifcate)	molar fraction (normalized)	Expanded uncertainty (k = 2) / mol%
Methane + n-butane			
CH_4 (CAS number: 74-82-8)	0.9896	0.98998	0.1500×10^{-2}
C_4H_{10} (CAS number: 106-97-8)	0.010017	0.01002	0.0030×10^{-2}
Methane+ isopentane			
CH_4 (CAS number: 74-82-8)	0.9797	0.98016	0.150×10^{-2}
iso-C_5H_{12} (CAS number: 78-78-4)	0.01983	0.01984	0.016×10^{-2}

Table 1: Composition expressed in molar fractions, relative expanded uncertainties (k = 2) for each component of the studied mixtures.

For preserving the traceability of speed of sound measurements through composition, the cylinders containing the samples were properly prepared before they were opened to fill the measuring system. Since, the mixtures can stratify inside the cylinder, modifying the composition, once extracted. The two gas cylinders were rolled for at least 10 hours before starting the measurements cycle in order to enhance turbulent gas mixing. Moreover, they were heated for two hours at their bottoms in order to trigger further mixing by convection. To prevent any impurities within the system, that might contaminate the

sample during measurement, the whole system (including the pressure vessel and the gas inlet line) was evacuated for a minimum of 5 days, while the pressure vessel temperature was raised to approximately 80 °C for degasing. Finally, the gas mixture at a pressure of approximately 0.1 MPa was made to flow both in the inlet line and the pressure vessel for a minimum of five minutes before the whole system was evacuated again.

5. Filling and measurement procedure

In order to avoid any further sample decomposition during pressure vessel filling a specific procedure, shown in figure 4, has been adopted. This procedure was carried out at each temperature change as, after completing the measurement along each isotherm, the system was emptied for safety reasons. The

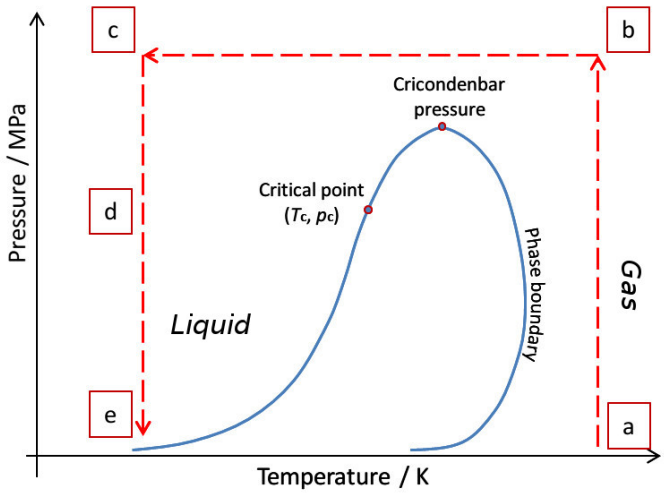

Figure 4: $p - T$ diagram of a typical natural gas with a scheme showing filling and measurement procedure.

pressure vessel is filled at ambient temperature ("a" in Fig. 4) until the pressure reaches a value higher than the maximum pressure on the saturation line, i.e. the cricondenbar pressure ("b" in Fig. 4). Then, the system is isobarically cooled to the temperature at which the measurement is to be carried out ("c" in Fig. 4). This ensures that the fluid can reach cryogenic temperatures without passing through the two-phase region, avoiding the separation of one of the mixture's components and thus keeping the gas composition homogeneous filling the pressure vessel. When the temperature of the system is stable, the first speed of sound measurement can be performed. After each measurement, the sample fluid is vented from the system to reduce the pressure while maintaining a constant temperature ("d" in Fig. 4). In this way the pressure is reduced, step by step, so as to cover the entire isotherm down to the minimum pressure (selected for each isotherm to avoid exceeding the phase boundary) ("e" in Fig. 4). For safety reasons, we preferred not to leave the liquefied gas stored in the pressure vessel overnight, in order to avoid any harmful consequences (e.g. due to a sudden increase in pressure caused by system overheating). For this reason, at the end of each isotherm, the system was completely vented and the filling procedure was repeated for the measurement along the next isotherm. The whole procedure described in this session takes about 15 to 18 hours to complete, since the cooling of the system alone

takes about 10 hours and changing from a given pressure to the next one, until reaching the equilibrium, takes more than 1 hour to complete.

6. Measurement repeatability and reproducibility

The repeatability of speed of sound experimental results was estimated by doing a second run of measurements along two isotherms. Since for both natural gas mixtures the measurements were carried out at temperatures of 100 K, 110 K, 120 K, 130 K, 140 K, 150 K and 160 K, we opted to repeat the measurements for the minimum and maximum temperatures within this range, in order to get the limit conditions of our interest. Hence, the measurements at 100 K and 160 K were repeated, after completing a full cycle of measurements at all other temperatures. Following this procedure, we estimated the reproducibility of the measurements for both mixtures to be 0.04 % (the largest value of repeatability was chosen to be more conservative).

In addition, another effect arising from potential decomposition of the sample fluid during the system's de-pressurisation have to be taken into account. In fact, once the fluid has been brought to the desired temperature, the system is thermostated and the gas is vented from the pressure vessel in order to switch from a higher to a lower pressure. During this process of venting from the pressure vessel to the atmosphere, an evaporation process normally takes place on the liquid/vapour separation surface within the inlet line. This leads to a possible separation of the lighter and heavier components of the mixture, resulting in a layer immediately below the liquid/vapour surface where the composition of the mixture is altered. Thus, it is essential to design the measuring system in such a way as to keep the surface where evaporation takes place as far as possible from the measuring cell. In particular, the gas inlet line into the pressure vessel is manufactured and sized with a series of bends so as to maximise the distance between the liquid/vapour surface and the point of entry into the pressure vessel. In addition, the presence of a heat shield, that can be cooled to cryogenic temperatures on the head of the pressure vessel, ensures that the evaporation surface remains outside the pressure vessel during the entire measuring process as well as during the venting of the system.

However, as the pressure is lowered, the level of the separation line can drop to a level where it would enter the pressure vessel. Consequently, the evaporation surface, and hence the volume of gas evaporating during venting, would no longer be negligible and could produce a change in fluid composition. Therefore, this effect would be gradually more evident as the pressure across each isotherm is reduced. In order to address this possibility and to include also the effects of a possible, even if minimal, decomposition of the mixture in the uncertainty analysis, additional reproducibility measurements at (100 and 160) K have been performed using an independent procedure for cooling and depressurizing the system, as opposed to that normally used for experimental measurements. This new procedure, shown in Fig. 5, is specifically meant to allow lower pressures to be reached directly, avoiding venting the gas from the pressure vessel during the descent.

The fluid is pressurized to supercritical pressure while it is at room temperature ("a" to "b" in Fig. 5). It is then cooled at constant pressure to a temperature just above the setpoint temperature ("c" in Fig. 5). This temperature is estimated using the derivative terms $\mathrm{d}p/\mathrm{d}T$ at constant density, provided by the

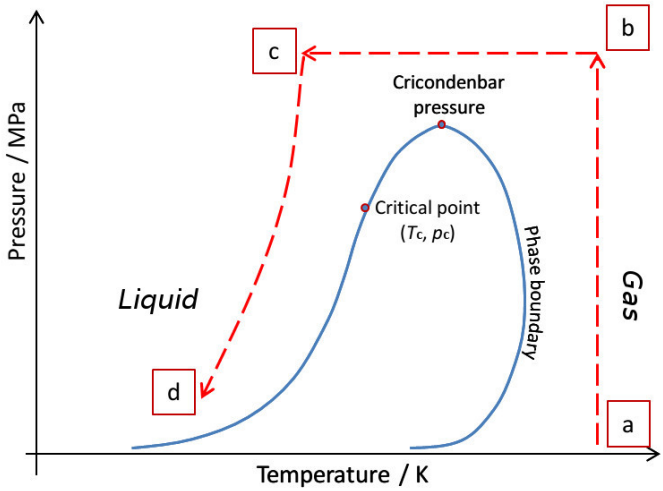

Figure 5: Principle of the flling and liquefaction procedure adopted for the reproducibility measurements at (100 and 160) K.

REFPROP software [13], developed by NIST (*National Institute of Standards and Technology*). This software is maintained by NIST's *Thermophysical Properties of Fluids Group* and is constantly updated to keep up to date with the performance and results delivered by introducing new fluids of industrial interest, new and updated experimental measurements and, in general, incorporating the latest developments coming from the scientific community. Then the pressure vessel is isolated and, thereafter, the system is further cooled down to the target temperature. Since the system is isolated, this cooling takes place at a constant volume causing at the same time a drop in the system pressure to the pressure required for the reproducibility determination. Using this technique, two measurements have been conducted at the thermodynamic points at (T = 160 K and p = 2 MPa) and at (T = 100 K and p = 4 MPa) ("d" in Fig. 5). By comparing these points with the corresponding two points obtained during the speed of sound measurements, a reproducibility of 0.057 % has been estimated. Again, the highest value was chosen, for being more conservative. Therefore, we assumed that any effects due to the decomposition of the mixtures during the venting and the depressurization of the system, already considered above for the calculation of repeatability, may be included in the reproducibility value. Nevertheless, we found it useful to include the value of reproducibility alongside the repeatability value in the uncertainty budget, in order to be sure to have totally accounted for the effects of a possible change in fluid composition.

7. Uncertainty analysis

The experimental speed of sound $w(T, p, X)$ is obtained by the independent measurements of both the acoustic path ΔL, and the time-of-flight τ, and it also depends on the measurements of the temperatures T, the pressures p, and the compositions, X of the gas mixtures. Beneath this basis, the uncertainty of the experimental measurements, can be estimated, as outlined in the GUM [27], by using the following expression for error propagation:

Uncertainty source	Contribution / %
Methane + n-butane	
Acoustic path length	0.026
Time of flight	0.005
Temperature	0.088
Pressure	0.082
Main component	0.13
Second component	0.003
Repeatability	0.041
Reproducibility	0.057
Relative expanded combined uncertainty (k=2)	< 0.35
Methane + isopentane	
Acoustic path length	0.026
Time of flight	0.005
Temperature	0.088
Pressure	0.063
Main component	0.12
Second component	0.013
Repeatability	0.041
Reproducibility	0.057
Relative expanded combined uncertainty (k=2)	< 0.30

Table 2: List of the uncertainty sources for the calculation of the overall expanded uncertainty (with k = 2) of speed of sound for two natural gas mixtures (methane + n-butane and methane + isopentane) for temperatures between (100 and 160) K and pressure up to 12 MPa.

$$\frac{\sigma(w)}{w} = \sqrt{\left(\frac{\sigma(\Delta L)}{\Delta L}\right)^2 + \left(\frac{\sigma(\tau)}{\tau}\right)^2 + \left(\frac{\sigma(T)}{w}\frac{\partial w}{\partial T}\right)^2 + \left(\frac{\sigma(p)}{w}\frac{\partial w}{\partial p}\right)^2 + \left(\frac{\sigma(X_1)}{w}\frac{\partial w}{\partial X_1}\right)^2 + \left(\frac{\sigma(X_2)}{w}\frac{\partial w}{\partial X_2}\right)^2 + R^2 + \epsilon^2}, \tag{12}$$

where R is the relative repeatability and ϵ is the reproducibility of the measurements, X_1 and X_2 are the molar fractions of the components of each gas mixture, while $\sigma(X_1)$ and $\sigma(X_2)$ are the expanded uncertainties (k = 2) associated with the mixture certificates provided by the VSL and listed in Table 1.

Table 2 shows the contributions to the relative combined expanded uncertainties of experimental speed of sound, $U_r(w)$ for both mixtures examined in this work. The uncertainties were first determined for each mesured state point, but eventually it has been decided to keep only the highest values among them for each mixture, obtaining uncertainty values of 0.35 % for the mixture containing n-butane and 0.3 % for that containing isopentane. The slight discrepancy between the two results is largely due to the pressure-related uncertainty contribution, given essentially to the sensitivity coefficient term of the speed of sound with respect to pressure. In fact, this term typically reaches the highest values for higher temperatures and for T = 160 K is about 28 % greater for the methane+n-butane mixture than that for the methane+isopentane mixture. The uncertainty associated with time-of-flight, $\sigma(\tau)$, coincides with twice the digital oscilloscope sampling interval, while the temperature uncertainty; $\sigma(T)$, is of 0.02 K, which is the uncertainty of the platinum resistance thermometers (PT100) used in this experiment. Similarly, the pressure uncertainty, $\sigma(p)$, is 0.025 MPa, namely the uncertainty of the temperature controlled pressure

transducer (Honeywell Super TJE) used during the experiment. Finally, the sensitivity coefficients related to temperature and pressure, $\partial w/\partial T$ and $\partial w/\partial p$, are obtained by fitting the experimental results.

8. Experimental results and comments

Speed of sound measurements have been carried out for two selected binary mixtures along seven isotherms from (100 to 160) K and for pressure up to 12 MPa. The two synthetic natural gas mixtures were supplied by VSL, with their calibration certificate. According to the supplier certification, their composition is 98.998 mol% methane + 1.0021 mol% n-butane, for the first mixture, and 98.016 mol% methane + 1.984 mol% isopentane, for the second one. For each isotherm, measurements started at the pressure of about 12 MPa, down to the lowest attainable pressure without the risk of exceeding the phase boundary. Table 3 shows the experimental results of speed of sound for both the gas samples.

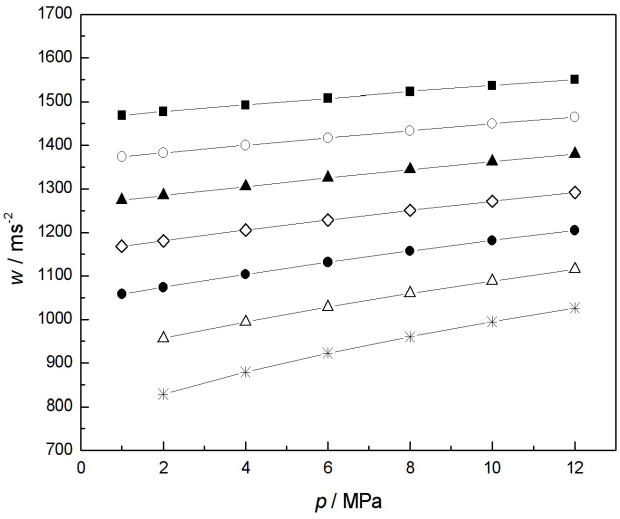

Figure 6: Experimental speeds of sound in methane+n-butane binary mixture as a function of pressure at temperatures between (100 and 160) K. ((■) T = 100 K; (○) T = 110 K; (▲) T = 120 K; (◇) T = 130 K; (●) T = 140 K; (△) T = 150 K; (✳)) T = 160 K.

Figure 6 plots the experimental speed of sound obtained for methane + n-butane; while in Fig. 7 results for methane+isopentane are depicted. For a sake of clearness of the charts, the speeds of sound have been adjusted to the temperatures of nominal isotherms. As shown, the speed of sound decreases with decreasing temperature and, similarly, reaches the lowest values with decreasing pressures. At the same time it is evident how, for both mixtures, the pressure dependence is more pronounced when the pressure of the fluid is low.

Since there are currently no available speed of sound experimental measurements for the two specific natural gas mixtures examined in this work, the obtained results will be of particular interest in validating the mathematical models used to calculate the thermodynamic properties of natural gases. Since this model accounts for many components, like: methane, nitrogen, carbon dioxide, ethane, propane, n-butane, isobutane, n-pentane, isopentane, n-hexane, n-heptane, n-octane, n-nonane, n-decane, hydrogen,

98.998 mol% methane + 1.0021 mol% n-butane					
T / K	p / MPa	w / m s^{-1}	T / K	p / MPa	w / m s^{-1}
100.05	0.92	1468.01	140.00	1.05	1059.18
100.03	2.05	1477.94	139.94	2.11	1076.52
99.98	3.93	1492.48	140.09	3.98	1102.49
100.04	6.10	1508.21	140.00	6.00	1131.69
100.06	7.91	1522.06	140.12	7.91	1155.22
99.97	9.92	1536.58	140.10	9.54	1175.44
100.02	11.09	1544.21	140.03	11.59	1199.82
110.13	0.93	1372.11	150.13	2.02	955.43
110.08	1.96	1382.04	150.07	4.08	994.67
110.12	3.93	1398.69	150.08	6.07	1028.68
109.94	6.04	1418.37	150.18	7.94	1056.83
110.09	7.61	1429.77	150.10	10.03	1087.88
109.99	9.51	1446.49	150.11	11.29	1104.94
109.98	11.93	1464.99			
119.76	0.87	1275.03	160.04	2.15	831.82
119.85	2.09	1287.27	159.91	4.10	882.05
119.89	3.89	1305.32	159.88	6.03	923.92
119.87	6.02	1326.87	159.90	8.19	964.47
119.78	8.03	1346.77	160.00	10.09	995.83
119.74	9.82	1363.20	159.89	12.48	1034.61
119.81	11.46	1376.92			
130.03	1.10	1168.80			
129.98	2.02	1180.96			
129.98	4.05	1206.22			
129.97	6.07	1229.69			
130.01	8.14	1252.08			
129.98	9.97	1271.46			
129.97	12.21	1294.00			

98.016 mol% methane + 1.984 mol% isopentane					
T / K	p / MPa	w / m s^{-1}	T / K	p / MPa	w / m s^{-1}
100.19	0.60	1475.88	140.22	2.14	1090.74
100.18	1.90	1485.96	140.07	3.06	1105.77
100.24	2.62	1490.79	140.04	4.05	1119.99
100.21	6.07	1516.17	139.96	8.01	1171.48
100.16	8.73	1534.94	140.03	9.02	1183.19
100.22	10.11	1544.22	139.99	11.65	1213.90
100.07	11.20	1552.65			
110.05	1.02	1385.35	150.07	2.06	979.33
110.04	2.03	1394.18	150.10	2.94	995.11
110.03	3.04	1402.70	150.09	6.01	1046.01
110.03	6.05	1427.94	150.10	8.03	1076.05
110.03	8.03	1443.73	150.09	9.06	1090.86
110.05	9.07	1451.63	150.04	11.59	1125.01
110.03	11.88	1473.42			
119.99	1.06	1289.33	159.94	2.95	878.19
120.01	2.00	1298.72	159.85	5.98	942.45
120.01	3.08	1309.33	160.22	8.03	976.39
120.04	6.09	1338.14	160.21	8.03	976.62
120.02	7.96	1355.25	159.93	9.05	996.65
120.01	9.03	1364.96	159.93	11.86	1040.54
119.98	11.86	1389.41			
130.03	1.06	1186.60			
130.03	2.05	1199.22			
130.01	3.01	1210.59			
130.08	6.13	1245.10			
130.02	9.00	1275.99			
130.06	11.90	1304.06			

Table 3: Experimental values of speed of sound in two binary mixtures of natural gas (98.998 mol% methane + 1.0021 mol% n-butane and 98.016 mol% methane + 1.984 mol% isopentane). The expanded combined relative uncertainty (k = 2) for speed of sound is $U_r(w) = 0.35$ % ($k = 2$) for methane + n-butane and $U_r(w) = 0.30$ % ($k = 2$) for methane + isopentane.

oxygen, carbon monoxide, water, hydrogen sulfide, helium, and argon, it is very difficult to obtain

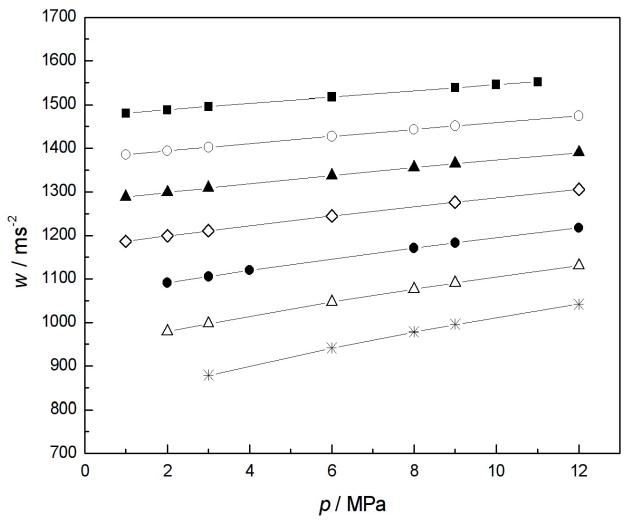

Figure 7: Experimental speeds of sound in methane+isopentane binary mixture as a function of pressure at temperatures between (100 and 160) K. ((■) T = 100 K; (○) T = 110 K; (▲) T = 120 K; (◇) T = 130 K; (●) T = 140 K; (△) T = 150 K; (✳) T = 160 K.

experimental measurement for all the possible combination and compositions. Thus, the mixture model implemented in GERG-2008 works using accurate equations of state in the form of fundamental equations for each component of the mixture coupled with specially developed binary functions of the components to take into account the residual behavior of the mixture. However, specific mixing rules are only available for some of the 21 components. With respect to the mixtures of methane + n-butane and methane + isopentane, the GERG-2008 model does not include any of them, due to a lack of experimental data (especially density and speed of sound) at the time of this publication. This lack of data has been partly overcome in recent years, leading to the possibility of publishing a new enhanced version of the GERG-2008 fundamental equation of state, namely the EOS-LNG equation of state. In this new model new binary-specific functions for methane + n-butane, methane + isobutane, methane + n-pentane, and methane + isopentane have been developed. A comparison between the new experimental results, which are the first available speed of sound values for these two mixtures, with the values calculated using GERG-2008 and EOS-LNG.

8.1. Methane + n-butane Speed of Sound results

For the 98.998 mol% methane + 1.0021 mol% n-butane mixture, the speed of sound was measured with an extended relative uncertainty (k = 2), $U_r(w)$= 0.35 %.

Fig. 8 and Fig. 9 plot the percentage deviations of the experimental measurement of speed of sound in the methane + n-butane mixture from the values calculated using the GERG-2008 and EOS-LNG models, respectively.

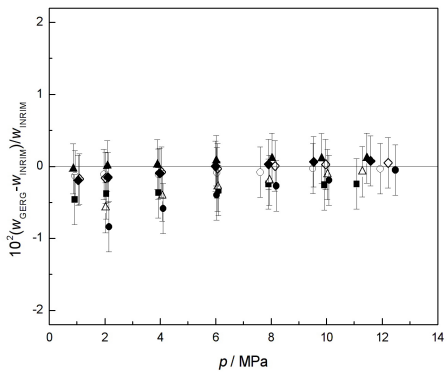

Figure 8: Deviations between experimental speeds of sound in methane + n-butane binary mixture and the GERG-2008 results for temperatures between (100 and 160) K and pressure up to 12 MPa. ((■) T = 100 K; (○) T = 110 K; (▲) T = 120 K; (◇) T = 130 K; (◆) T = 140 K; (△) T = 150 K; (●) T = 160 K.

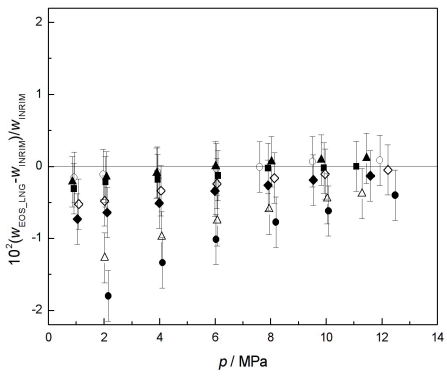

Figure 9: Deviations between experimental speeds of sound in methane + n-butane binary mixture and the EOS-LNG results for temperatures between (100 and 160) K and pressure up to 12 MPa. ((■) T = 100 K; (○) T = 110 K; (▲) T = 120 K; (◇) T = 130 K; (◆) T = 140 K; (△) T = 150 K; (●) T = 160 K.

Surprisingly, in both cases the most dated versions of the used models, GERG-2008 and REFPROP (version 9), appear more consistent with the experimental results than the most updated models, EOS-LNG and REFPROP (version 10). For all four of these comparisons, the experimental points are dispersed around the zeros of the graphs, meaning that they are distributed around the values predicted by all of the equations of state under investigation. Nevertheless, the dispersion of these data in the case of GERG-2008 and REFPROP (version 9) is significantly smaller compared to that of the most up-to-date models. Especially at the lowest temperatures, the experimental results are all in agreement with the values predicted by both GERG-2008 and REFPROP (version 9) and become unconsistent only for the lowest pressures (2, 4, and 6) MPa for the isotherms (150 and 160) K, with scatter values ranging from (-0.4 to -0.8) %.

In contrast, the deviations from the values predicted by the most updated models, EOS-LNG and REFPROP (version 10), are always larger than those of the earlier model data. In this case, the experimental results are not consistent for temperatures in the range of (140 to 160) K at any chosen pressure, with deviation amounts up to 1.8 %. In this frame, the EOS-LNG model seems to perform slightly better than REFPROP (version 10) for temperatures from (100 to 120 K), which are all in agreement with the predicted values, while for T between (130 and 140) K the consistency between the values occurs only for the highest pressures, fro (6 to 12) MPa. In contrast, compared to the results obtained with REFPROP (version 10), the experimental speeds of sound are more dispersed. In this case, the model reproduces

our results only at temperatures of (110 and 120) K, at T = 100 K for pressures up to 6 MPa and at T = 130 K, only for higher pressures, p = (10 and 12) MPa.

8.2. Methane + isopentane Speed of Sound results

The same comparisons between experimental results and expected values from the reference equations of state have been performed for measurements in the 98.016 mol% methane + 1.984 mol% isopentane mixture. In this case, the extended relative uncertainty (k = 2) has been estimated as $U_r(w)$= 0.3 %. Fig. 10 and Fig. 11 report the deviations from the predictions of GERG-2008 and EOS-LNG, respectively, while in Fig. 12 and Fig. 13 deviations from REFPROP version (version 9) and REFPROP (version 10) are plotted.

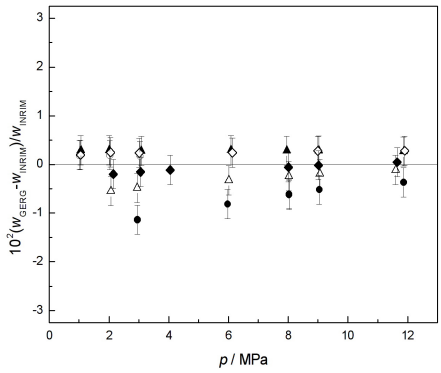

Figure 10: Deviations between experimental speeds of sound in methane + isopentane binary mixture and the GERG-2008 results for temperatures between (100 and 160) K and pressure up to 12 MPa. ((■) T = 100 K; (○) T = 110 K; (▲) T = 120 K; (◇) T = 130 K; (◆) T = 140 K; (△) T = 150 K; (●) T = 160 K.

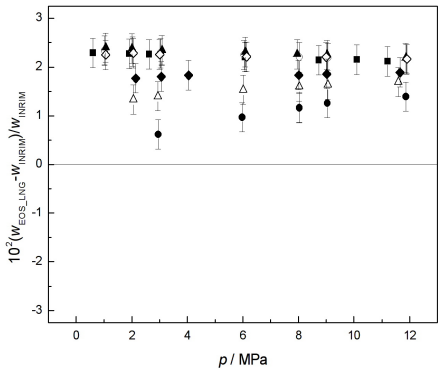

Figure 11: Deviations between experimental speeds of sound in methane + isopentane binary mixture and the EOS-LNG results for temperatures between (100 and 160) K and pressure up to 12 MPa. ((■) T = 100 K; (○) T = 110 K; (▲) T = 120 K; (◇) T = 130 K; (◆) T = 140 K; (△) T = 150 K; (●) T = 160 K.

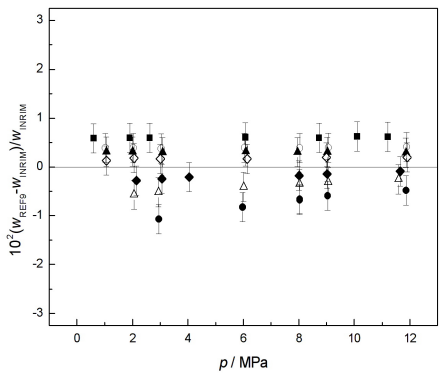

Figure 12: Deviations between experimental speeds of sound in methane + isopentane binary mixture and the REFPROP (version 9) results for temperatures between (100 and 160) K and pressure up to 12 MPa. ((■) T = 100 K; (○) T = 110 K; (▲) T = 120 K; (◇) T = 130 K; (◆) T = 140 K; (△) T = 150 K; (●) T = 160 K.

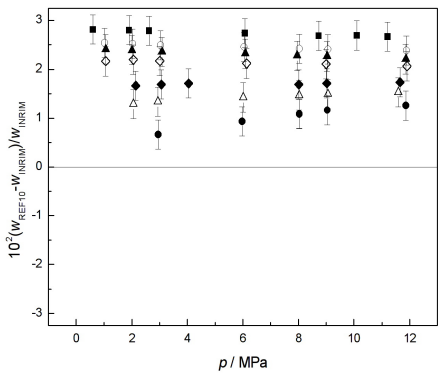

Figure 13: Deviations between experimental speeds of sound in methane + isopentane binary mixture and the REFPROP (version 10) results for temperatures between (100 and 160) K and pressure up to 12 MPa. ((■) T = 100 K; (○) T = 110 K; (▲) T = 120 K; (◇) T = 130 K; (◆) T = 140 K; (△) T = 150 K; (●) T = 160 K.

For this second set of results, comparisons with the equations of state make even more evident the

difference, already seen for the previous mixture, between the predictions of the different models. In fact, the GERG-2008 is the model which better represents the values obtained from the experimental measurements, which are largely in agreement, especially for the lowest temperatures, from (110 to 140) K. At 150 K, the results are consistent for pressures from (8 to 12) MPa, while only the measurements performed at T = 160 K are not comparable with the predicted values. On the other hand, the speeds of sound calculated by REFPROP (version 9) are consistent with the experimental measurements only for temperatures at (140 and 130) K, while the measurements carried out at any other temperature are not comparable with the results given by the model.

However, the most updated models both provide results that show significant inconsistencies with the experimental values. In fact, the expected results obtained from both EOS-LNG and REFPROP (version 10) deviate up to 2.4 %, for EOS-LNG, and about 3 %, for REFPROP (version 10). Moreover, also in this case, the dispersion of the experimental values around the expected results obtained using the reference equations is much larger for novel models while it is narrower for the older ones.

9. Conclusions

Accurate speed of sound measurements in two synthetic natural gas binary mixtures (98.998 mol% methane + 1.0021 mol% n-butane and 98.016 mol% methane + 1.984 mol% isopentane) have been carried out along seven isotherms from T =(100 to 160) K at pressures up to about 12 MPa, using an ultrasonic sensor, whose working principle is based on the duoble pulse echo technique. The experimental results have been compared with the GERG-2008 equation of state, which is the ISO standard for the calculation of thermodynamic properties of natural gas mixtures, the NIST REFPROP model (version 10), which is widely used for the study of a broad variety of industrial fluids and fluids of scientific interest.

It is to be noted that the default pure fluid equations of state used in REFPROP are not the same as those used in the GERG-2008 model. In fact, the GERG-2008 expressions for the pure fluids are shorter, less complex, and faster, but slightly less accurate. In addition, mixing rules used in REFPROP have been updated to those published in 2019 by Thol *et al.*, with the publication of a new equation of state for natural gas binary mixtures, EOS-LNG, whereas in the previous version of REFPROP (version 9), the mixing rules were the same as those used by the GERG-2008 model.

Therefore, for these reasons, the authors decided to perform further comparisons with both the values predicted by the EOS-LNG model and those provided by REFPROP (version 9). These comparisons point out that, the more dated models, GERG-2008 and REFPROP (version 9), are in better agreement with the experimental speeds of sound obtained in this work. On the other hand, comparisons with the more up-to-date models, REFPROP (version 10) and EOS-LNG, i.e., the enhanced version of GERG-2008, show larger deviations. In particular, for the methane + n-butane mixture the dispersion of the experimental data around the expected values is larger and, although for lower temperatures they are consistent, most of the measurements are not in agreement with the results returned by these models. This divergence appears more apparent when analyzing the dispersion plots for the methane + isopentane mixture. In this case, while comparisons with GERG-2008 and REFPROP (version 9) show agreement with most of the experimental results, particularly for the GERG-2008 equation of state. Conversely, comparing these

results with the expected values provided by the EOS-LNG model and REFPROP (version 10) deviations of up to 3 % can be found.

In conclusion, it is shown that the most up-to-date models appear to predict less effectively the experimental speed of sound values obtained in this work. This finding is, most likely, due to the introduction into these equations of state of new mixing rules for the binary mixtures examined for these measurements. In fact, the coefficients of these mixing rules were calculated when no experimental speed of sound measurements were yet available for mixtures of methane and n-butane and methane and isopentane. Therefore, the novel experimental speeds of sound here submitted may be of interest in further adjusting and improving of the cited mathematical models, for the two specific binary mixtures examined in this work.

Acknowledgements

This project (16ENG09-LNG3) has received funding from the EMPIR programme co-financed by the Participating States and from the European Union's Horizon 2020 research and innovation programme.

References

[1] Alam, M. S., Paramati, S. R., Shahbaz, M., Bhattacharya, M. (2017). Natural gas, trade and sustainable growth: empirical evidence from the top gas consumers of the developing world. Applied Economics, 49(7), 635-649

[2] Dudley, B. (2018). BP energy outlook. Report–BP Energy Economics: London, UK, 9.

[3] Ahmadi, P., Chapoy, A., Tohidi, B. (2017). Density, speed of sound and derived thermodynamic properties of a synthetic natural gas. Journal of Natural Gas Science and Engineering, 40, 249-266.

[4] Estrada-Alexanders, A. F., Trusler, J. P. M., Zarari, M. P. (1995). Determination of thermodynamic properties from the speed of sound. International journal of thermophysics, 16(3), 663-673.

[5] Trusler, J. P. M., Zarari, M. (1992). The speed of sound and derived thermodynamic properties of methane at temperatures between 275 K and 375 K and pressures up to 10 MPa. The Journal of Chemical Thermodynamics, 24(9), 973-991.

[6] Lin, C. W., Trusler, J. P. M. (2012). The speed of sound and derived thermodynamic properties of pure water at temperatures between (253 and 473) K and at pressures up to 400 MPa. The Journal of chemical physics, 136(9), 094511.

[7] Cavuoto, G., Lago, S., Giuliano Albo, P. A. (2021). Towards a new transfer standard for speed of sound measurements in liquids at cryogenic temperatures. Measurement, 180, 109526.

[8] Eisenbach, T., Scholz, C., Span, R., Cristancho, D., Lemmon, E. W., Thol, M. (2021). Speed-of-Sound Measurements and a Fundamental Equation of State for Propylene Glycol. Journal of Physical and Chemical Reference Data, 50(2), 023105.

[9] Trusler, J. M., Lemmon, E. W. (2017). Determination of the thermodynamic properties of water from the speed of sound. The Journal of Chemical Thermodynamics, 109, 61-70.

[10] Starling, K. E., Savidge, J. L. (1992). Compressibility factors of natural gas and other related hydrocarbon gases. American Gas Association, Operating Section.

[11] Kunz, O., Wagner, W. (2012). The GERG-2008 wide-range equation of state for natural gases and other mixtures: an expansion of GERG-2004. Journal of chemical and engineering data, 57(11), 3032-3091.

[12] Thol, M., Richter, M., May, E. F., Lemmon, E. W., Span, R. (2019). EOS-LNG: a fundamental equation of state for the calculation of thermodynamic properties of liquefied natural gases. Journal of Physical and Chemical Reference Data, 48(3), 033102.

[13] Lemmon, E. W., Bell, I. H., Huber, M. L., McLinden, M. O. (2018). NIST Standard Reference Database 23: Reference Fluid Thermodynamic and Transport Properties-REFPROP, Version 10.0, National Institute of Standards and Technology. Standard Reference Data Program, Gaithersburg.

[14] Kunz, O., Klimeck, R., Wagner, W., Jaeschke, M. (2007). The GERG-2004 wide-range equation of state for natural gases and other mixtures.

[15] Cavuoto, G., Lago, S., Giuliano Albo, P. A., Serazio, D. (2020). Speed of sound measurements in liquid methane (CH4) at cryogenic temperatures between (130 and 162) K and at pressures up to 10 MPa. The Journal of Chemical Thermodynamics, 142, 106007.

[16] Preston-Thomas, H. (1990). The International Temperature Scale of 1990(ITS-90). metrologia, 27(1), 3-10.

[17] Goodwin, A., Marsh, K. N., Wakeham, W. A. (2003). Measurement of the thermodynamic properties of single phases. Elsevier.

[18] Benedetto, G., Gavioso, R. M., Giuliano Albo, P. A., Lago, S., Ripa, D. M., Spagnolo, R. (2005). Speed of sound in pure water at temperatures between 274 and 394 K and at pressures up to 90 MPa. International journal of thermophysics, 26(6), 1667-1680.

[19] Javed, M. A., Baumhogger, E., Vrabec, J. (2019). Thermodynamic speed of sound data for liquid and supercritical alcohols. Journal of Chemical and Engineering Data, 64(3), 1035-1044.

[20] Lin, C. W., Trusler, J. P. M. (2014). Speed of sound in (carbon dioxide + propane) and derived sound speed of pure carbon dioxide at temperatures between (248 and 373) k and at pressures up to 200 mpa. Journal of Chemical and Engineering Data, 59(12), 4099-4109.

[21] Meier, K., Kabelac, S. (2012). Thermodynamic properties of propane. IV. Speed of sound in the liquid and supercritical regions. Journal of Chemical and Engineering Data, 57(12), 3391-3398.

[22] Trusler, M. (1991). Physical acoustics and metrology of fluids. CRC Press.

[23] Trusler, M. (1991). Physical acoustics and metrology of fluids. CRC Press.

[24] Giuliano Albo, P. A., Lago, S., Romeo, R., Lorefice, S. (2013). High pressure density and speed-of-sound measurements in n-undecane and evidence of the effects of near-field diffraction. The Journal of Chemical Thermodynamics, 58, 95-100.

[25] Corruccini, R. J., Gniewek, J. J. (1961). Thermal expansion of technical solids at low temperatures: A compilation from the literature (Vol. 29). US Department of Commerce, National Bureau of Standards.

[26] International Organization for Standardization (ISO), ISO 6143:2001 — Gas analysis — Comparison methods for determining and checking the composition of calibration gas mixtures. (2001)

[27] International Organization for Standardization. (2008). Uncertainty of Measurement: Guide to the Expression of Uncertainty in Measurement (GUM: 1995). Propagation of Distributions Using a Monte Carlo Method. International Organisation for Standardization.